

Selection of a Minimal Suboptimal Set of EFMs for Dynamic Metabolic Modelling

M. Maton* Ph. Bogaerts** A. Vande Wouwer*

* *Systems, Estimation, Control and Optimization Laboratory,
University of Mons. 31 Boulevard Dolez, Mons 7000, Belgium.*

** *Université Libre de Bruxelles, Brussels School of Engineering,
3BIO-BioControl. Av. F.D. Roosevelt 50 C.P. 165/61, Brussels 1050,
Belgium.*

Abstract: Mathematical modelling supports the understanding of basic biological mechanisms and is the basis for bioprocess simulation, prediction, control and optimization. Dynamic macroscopic models can be derived from the concept of elementary flux modes (EFMs), which provide a comprehensive representation of all possible pathways through a metabolic network. As the number of EFMs drastically increases with the size of the metabolic network, a procedure to reduce the number of EFMs and select the most informative ones is required. For this purpose, this study proposes a methodology to select a minimal suboptimal set of elementary flux modes allowing the development of reduced macroscopic models. The algorithm is divided into two steps. First, the concept behind the cosine-similarity algorithm is extended for a large number of EFMs to cut the initial set by removing all the collinear modes. Next, the algorithm is used to extract only the most informative modes from the reduced set by means of a series of optimization problems. The algorithm performance is illustrated with datasets from hybridoma cultures in batch and perfusion modes, and two metabolic networks with different levels of description.

Copyright © 2021 The Authors. This is an open access article under the CC BY-NC-ND license (<http://creativecommons.org/licenses/by-nc-nd/4.0>)

Keywords: Macroscopic modelling, metabolic flux analysis, elementary flux modes, model reduction

1. INTRODUCTION

In the last decades, mammalian cell cultures have been widely used in laboratory settings particularly in the field of vaccine research, cancer treatment and protein therapeutics. Cells derived from animals, especially mammals, have become fundamental to biomanufacturing of a large number of biologics including monoclonal antibodies (Sidoli et al., 2004; Niklas and Heinzle, 2012), viral vaccines (Vester et al., 2010) and numerous proteins employed in the treatment of genetic diseases. For industrial purposes, large-scale cell cultures present a great interest despite some engineering challenges (Niu et al., 2013). To tackle those issues and achieve high productivity and better quality products, the development of accurate dynamical models describing the metabolism of the cell shows a meaningful added value, as the efficiency of these processes can be further improved by means of model-based optimization and control strategies. For this purpose, several techniques have emerged over the years among which methods for deriving macroscopic models from intracellular information contained in detailed metabolic networks. Some of them are based on the concept of elementary flux modes or extreme pathways (Stelling et al., 2002), a notion consistent with the biological knowledge about the organism (Gao et al., 2007) and which allows translating the metabolic network into macroscopic bioreactions connecting extracellular substrates to products. However, a major problem encountered when using this approach is

a combinatorial explosion in the number of EFMs with the size of the metabolic network. Different approaches have been proposed to tackle this issue, including the computation of a minimal set of EFMs without enumerating all of them (Jungers et al., 2011; Machado et al., 2012) and the selection of subsets of EFMs as candidate macro-reactions. Following the latter approach, (Provost and Bastin, 2004; Zamorano et al., 2013) introduce additional constraints related to cell-specific uptake- or secretion rates so as to reduce the dimensionality of the solution space and develop dynamic models. (Song and Ramkrishna, 2009) demonstrate that the number of EFMs can be reduced by projection of the modes into yield space. (Naderi et al., 2010) depict a simplified metabolic network by removing all insignificant fluxes. In (Soons et al., 2010, 2011), an optimization criterion compromising error, efficiency of the modes, and model size is defined and EFMs are selected based on ranking or controlled random search. A study conducted by (Song et al., 2013) suggests how to reduce the number of EFMs by grouping them into clusters and computing an average EFM for each one. (Hebing et al., 2016) propose a method which allows reducing the set of EFMs by using a cosine-similarity algorithm followed by the definition of a multi-objective genetic algorithm to find a suitable set of EFMs. (Baroukh and Bernard, 2016) suggest methods based upon dynamic metabolic flux analysis (DMFA), flux balance analysis (FBA) and its extension, dynamical flux balance analysis (DFBA). Recently, (Abbate et al., 2019) have formulated a linear

optimization problem in order to select the best set of EFMs based on a relaxation criterion. The present study extends this latter work to include a more efficient selection criterion to face larger sets of EFMs.

More specifically, this study proposes an algorithm called Reducer of Elementary Modes (REM) in order to shorten the computation time and select only the most informative modes. First of all, the cosine-similarity algorithm introduced in (Hebing et al., 2016) is extended to cut the initial set of EFMs by removing all the collinear modes. Then, the methodology is pursued to extract only the most informative modes from the reduced set by means of a series of optimization problems. The algorithm works efficiently for metabolic networks with size around 100 reactions, which is typically the size of networks considered in most studies aiming at the derivation/reduction of dynamic models. In that respect, a minimal suboptimal set of EFMs is obtained and can be directly used for the development of macroscopic models.

This paper is organized as follows. The next section encompasses the problem statement and introduces the main concepts relative to the metabolic network analysis. The reduction algorithm is discussed in section 3. Section 4 presents the results of the test case studies. Experimental data of hybridoma cultures in batch and perfusion modes are analysed on the basis of two metabolic networks of different sizes and the outcomes of the reduction algorithm. Finally, conclusions are drawn in section 5.

2. PROBLEM STATEMENT

As defined in (Nelson and Cox, 2008), the cell metabolism is a set of enzyme-catalyzed transformations of organic molecules taking place in a living cell and forming metabolic pathways. The interconnection of such pathways devises a so-called metabolic network of biochemical reactions.

In metabolic engineering, a metabolic network is represented by a $m \times n$ stoichiometric matrix N where m stands for the number of internal metabolites and n corresponds to the number of reactions. With the purpose of analysing a network, the principle of mass conservation of internal metabolites is applied and accounting for the pseudo-steady state assumption, we obtain an homogeneous system of linear equations :

$$N \cdot \underline{v} = 0 \quad (1)$$

where $\underline{v} \in \mathbb{R}^n$ is the vector of network fluxes, also called the extreme rays of the network. Moreover, network fluxes are often constrained to positivity assuming that the direct reactions prevail over their reverse counterparts :

$$\underline{v} \geq 0 \quad (2)$$

Henceforth, system (1) under the positivity constraint (2) constitutes a problem of non-negative linear algebra or convex analysis whose solution space is a polyhedral cone in the positive orthant.

To tackle this concern, a non-decomposability constraint may be added to define a finite set of flux distributions. To that extent, the concept of elementary flux modes is introduced and can be interpreted as the simplest metabolic pathways connecting substrates to products without accumulation of metabolites. Therefore, these EFMs represent the edges of the polyhedral cone constructed by the intersection of the hyperplanes defined by the rows of N . In

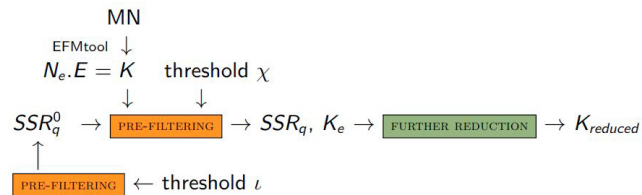


Fig. 1. The reduction procedure - the REM algorithm

the last decades, some techniques have been highlighted to compute the elementary flux modes, one of them being implemented in the popular toolbox EFMtool (Terzer and Stelling, 2008).

In addition, constraints relative to the measurements of extracellular fluxes can be defined through the so-called stoichiometric matrix of extracellular measurements N_e . This is a $m_e \times n$ matrix where m_e stands for the number of extracellular measurements.

In this study, the concept of EFMs is used to translate the metabolic network into macroscopic bioreactions in order to derive dynamic macroscopic models particularly useful in estimation and control. Nevertheless, for large metabolic networks, a combinatorial explosion in the number of elementary flux modes is observed justifying the use of reduction methods of the initial set of the modes.

3. REDUCTION ALGORITHM

This section is devoted to the reduction algorithm used to select a minimal suboptimal set of EFMs, denoted $K_{reduced}$ from an initial set K . The REM algorithm is introduced as an iterative method based on the optimization problem :

$$SSR_q = \sum_{k=1}^M \left(\|K_e \underline{\phi}(t_k) - \underline{v}_m(t_k)\|_2^2 \right) \quad (3)$$

$$\min_{\underline{\phi}(t_k)} SSR_q \quad s.t. \quad \underline{\phi}(t_k) \geq 0 \quad (4)$$

where $\underline{v}_m(t_k)$ is the vector of uptake and excretion rates for every time-step t_k obtained from the measured concentration profiles by means of smoothing splines and differentiation methods and $\underline{\phi}(t)$ represents a time-varying decomposition of the flux $\underline{v}_m(t)$ into a reduced set of modes stored in K_e . SSR_q is the sum of squared residuals and determines if the observed phenotypes are part of the solution space.

3.1 Pre-filtering of the Initial Set of EFMs

The first step of the REM algorithm relies on the concept of cosine-similarity developed in (Hebing et al., 2016). It performs a pre-reduction of the set of EFMs and is likely to become necessary when this set is large. Basically, the method can be broken down into two steps: (i) a reduction step based on a collinearity test and the value of a threshold χ allowing the cut and (ii) a validation step based on the formulation of an optimization problem. The first step consists in collinearity tests between the elementary flux modes, i.e., if the cosine of the angle between the extreme rays is larger than a defined threshold χ , then the elementary modes are oriented in the same direction and are redundant. The redundant modes are

thus eliminated and the remaining modes are stored in the reduced matrix K_e . In the second step, a comparison is achieved between the value of the indicator SSR_q resulting from the optimization problem formed by Eq. 3 and Eq. 4 and SSR_q^0 , defined as the best value of the indicator when all the EFMs are considered without any reduction, i.e. when the complete matrix K is considered (threshold $\chi = 1$):

$$|SSR_q^0 - SSR_q| < tol_1 \quad (5)$$

In this expression, tol_1 is a tolerance, and if the above inequality is not satisfied, the threshold χ defined in the previous step induces the removal of essential informative modes. To complete the algorithm, the approximation of SSR_q^0 has to be considered. Indeed, the value of SSR_q^0 can be easily computed for small metabolic networks, but becomes a problem for larger metabolic networks. The approach is again a 2-step process. The first step is a reduction procedure based on the cosine-similarity algorithm, where a threshold ι is a priori selected in order to comprise the following objectives :

- to be close enough to one in order to keep the valuable information contained in the initial set of elementary flux modes ;
- to be far enough from one to obtain a smaller matrix of EFMs and to reduce the computation time.

The value of this threshold ι is randomly selected but adjusted by means of the second step, which is based on the optimization problem composed of Eq. 3 and Eq. 4. It consists in analysing the value of SSR_q associated to the threshold defined previously (ι) and the value of SSR_q associated to an increased threshold by an increment ($\iota + \delta$). If the values of the successive SSR_q become identical after a number of iterations, SSR_q^0 is assumed to be correctly approximated.

3.2 Further Reduction

To further reduce the number of EFMs and select a minimal set of bioreactions, the second step of the REM algorithm considers as inputs the reduced matrix of elementary flux modes K_e , the associated value of SSR_q and the target number of EFMs after the completion of the reduction procedure. The output is then a minimal set of EFMs under a matrix form, $K_{reduced}$. The method consists in randomly removing an elementary mode using a random number generator and formulating the optimization problem given by Eq. 3 and Eq. 4 where matrix K_e represents the corresponding candidate matrix of EFMs.

If the updated value of the indicator (SSR_q^*) is relatively close to the value of the indicator coming from the pre-filtering (SSR_q), then the EFM under question is definitely discarded. Otherwise, the EFM is kept because it contains valuable information. This consists in checking the following inequality:

$$|SSR_q^* - SSR_q| < tol_2 \quad (6)$$

where tol_2 represents a tolerance. The algorithm carries on until the number of EFMs reaches the target number. It is worth noting that the smaller the target set, the larger the tolerance.

Whereas the cosine-similarity algorithm allows a geometric interpretation of the EFMs selection process, the second

step of the REM algorithm mostly targets the reproduction of the measured data. The risk entailed in this procedure is that an elementary flux mode representative of some key biological process could be eliminated if the rest of the EFMs achieves a faithful reproduction of the measured data. Some sensitivity analysis can be performed by running the REM algorithm a few times and examining the variability in the resulting sets of EFMs. The global procedure is illustrated in Fig. 1.

4. APPLICATION TO HYBRIDOMA CELL CULTURES IN PERFUSION

To illustrate this study, experimental data from hybridoma cell line HB58 producing antibodies type IgG1 are exploited. It involves four different cell cultures in perfusion from which on-line measurements are available. The information relative to the cell line, the media, the bioreactor operation mode and the analysis methods are described in (Niu et al., 2013). Two metabolic networks are considered, with different levels of details, and the REM algorithm is used to reduce the initial set of EFMs to a small subset capable of reproducing the measured data.

4.1 Small Metabolic Network

The first metabolic network includes 24 reactions representing the central metabolism of hybridoma cells and is presented in (Abbate et al., 2019). As depicted in Fig. 1, the first step of the methodology consists in computing the matrix E of EFMs by means of EFMtool. As discussed in Sec. 2, this requires the definition of the stoichiometric matrix N . In addition, we consider five extracellular measurements, i.e. glucose, lactate, glutamine, ammonia and alanine. As discussed in (Provost and Bastin, 2004), experimental measurements are used to deduce the stoichiometry of the macro-reactions. Henceforth, the matrix K is obtained as follows :

$$K = N_e \cdot E \quad (7)$$

In this case study, 11 elementary flux modes are obtained inducing 10 possible macro-reactions (two EFMs are identical). The number of EFMs is therefore quite small and the linear optimization problem developed in (Abbate et al., 2019) can be formulated easily. The number of combinations of 5 bioreactions among 11 EFMs is explored and the linear optimization problem is solved 462 times. The best combination is obtained after a short computation time. In order to test the REM algorithm, this reduction is repeated here. Table 1 and Fig. 2 (left colorbar) present the results provided by the pre-filtering. In this case, because the number of EFMs is small, the value of SSR_q^0 can be directly computed.

Table 1. Results of the pre-filtering step

Threshold	# EFM	SSR_q	SSR_q^0
1.000	10	0.21530797	SSR_q^0
0.980	9	0.21530797	
0.975	8	0.21531374	
0.970	7	0.22722035	
0.960	5	0.43080000	
0.940	3	0.68230000	

Admitting a slight tolerance, the threshold of 0.975 is selected which allows discarding two EFMs. The second

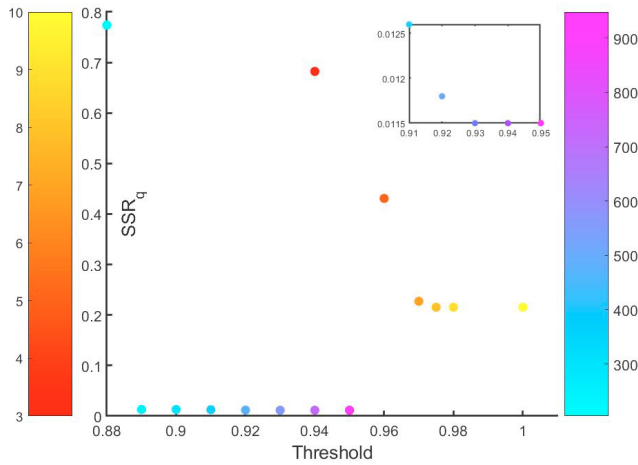


Fig. 2. Results of the pre-filtering for the small metabolic network of 24 reactions (left colorbar) and for the metabolic network of 70 reactions (right colorbar)

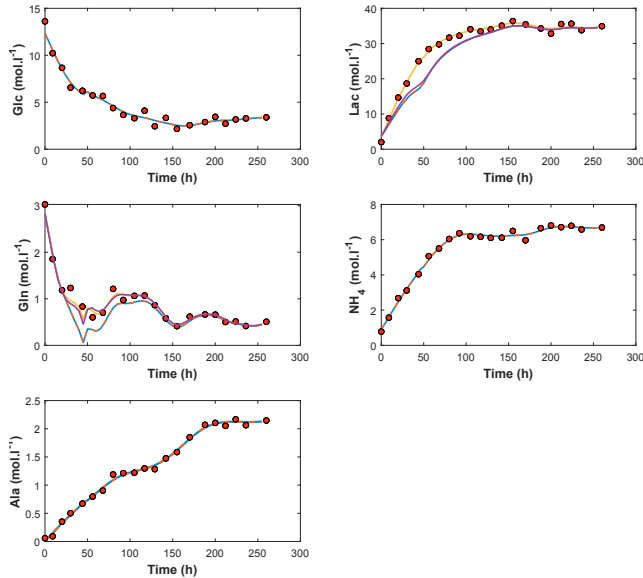


Fig. 3. Time evolution of the measured concentrations in dataset 4 by integration of the ϕ signals computed through the method proposed in (Abbate et al., 2019) (dark blue line) and the REM algorithm (dark orange line) - comparison with the REM results obtained with a larger metabolic network with 70 reactions and either 5 (yellow line) or 22 extracellular measurements (purple line).

step of the algorithm is then achieved with a target number of EFMs equal to 5. Indeed, it is known that m_e bioreactions are enough to fully explain the experimental data (Provost and Bastin, 2004). The results are presented in Fig. 3 as well as the results provided by the linear optimization problem formulated in (Abbate et al., 2019) for comparison purposes. This figure presents experimental data from dataset 4 and shows that both algorithms give the same results, thus validating the REM algorithm. The macroscopic model is described by the following dynamic mass-balance equations:

$$\frac{dGlc}{dt} = -\phi_1 X - 2\phi_4 X - \phi_5 X + D(Glc_{in} - Glc) \quad (8)$$

$$\frac{dLac}{dt} = 2\phi_1 X + \phi_2 X + 2\phi_4 X - DLac \quad (9)$$

$$\frac{dGln}{dt} = -\phi_2 X - \phi_3 X - 3\phi_4 X + D(Gln_{in} - Gln) \quad (10)$$

$$\frac{dN}{dt} = 2\phi_2 X + \phi_3 X + \phi_4 X - DN \quad (11)$$

$$\frac{dAla}{dt} = \phi_3 X + D(Ala_{in} - Ala) \quad (12)$$

where Glc_{in} , Gln_{in} and Ala_{in} are the concentrations of glucose, glutamine and alanine in the feed stream, D is the dilution rate and X is the biomass. This model is identical to the one obtained in (Abbate et al., 2019).

4.2 More Detailed Metabolic Network

A more detailed network (Fernandes de Sousa et al., 2015) including glycolysis, tricarboxylic acid cycle, amino acids metabolism, biomass and antibody synthesis is now considered. The network contains 70 reactions and 44 internal metabolites. In the following sections, two different cases are addressed. First, 22 extracellular measurements are considered. Second, only five extracellular measurements, identical to the ones considered in Sec. 4.1, are accounted for. For both cases, the first step of the procedure consists in computing the matrix of elementary flux modes, noted E. In this case, the number of EFMs amounts to 22563 making difficult the use of existing methods, especially the linear optimization problem introduced in (Abbate et al., 2019). For this purpose, reduction algorithms are essential and the REM algorithm is applied.

22-measurement case A prior step consists in evaluating the stoichiometry of the macro-reactions by exploiting Eq. 7. As mentioned in Sec. 3.1, to avoid computational issues, an approximation of the value of SSR_q^0 is needed.

Table 2. Cosine-similarity algorithm's results

Threshold	# EFM	SSR_q	
0.990	2643	*	
0.980	2221	*	
0.970	1636	*	
0.960	1227	*	
0.950	948	0.0115	$\iota^{+4\delta} SSR_q \approx SSR_q^0$
0.940	723	0.0115	$\iota^{+3\delta} SSR_q$
0.930	555	0.0115	$\iota^{+2\delta} SSR_q$
0.920	476	0.0118	$\iota^{+\delta} SSR_q$
0.910	369	0.0126	ιSSR_q
0.900	299	0.0129	
0.890	246	0.0129	
0.880	204	0.7740	

The key point is the selection of an adequate threshold to reduce the initial set of EFMs to a (much) smaller subset. As shown in Table 2 and Fig. 2 (right colorbar), a candidate threshold is 0.910 leading to a reduced matrix of 369 EFMs. The value of the threshold is increased (by an increment δ) and the evolution of SSR_q is monitored. In the present case, the value SSR_q plateaus after a few iterations and SSR_q^0 can be approximated at 0.0115. In view of the tiny difference with the level just below, at 0.0118, a subset of 476 EFMs can be adopted to define the

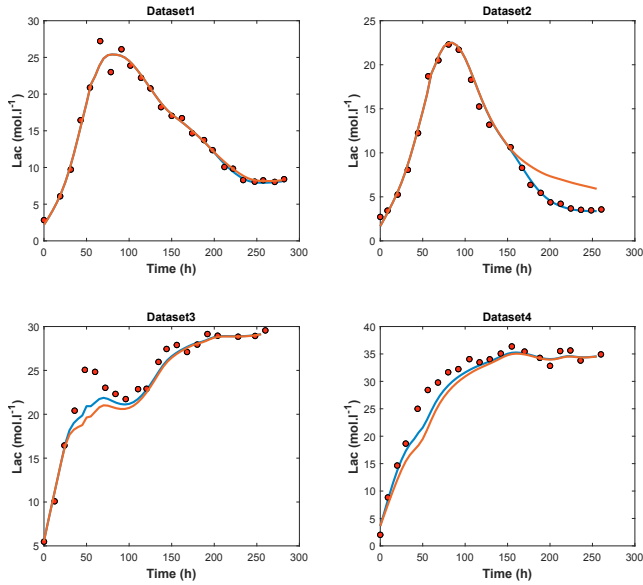


Fig. 4. Time evolution of the lactate concentration - results of step 1 (blue line) and step 2 (orange)

matrix K_e . The next step in the algorithm is the definition of a target number of 22 EFMs to explain the data (corresponding to the number of extracellular species that can be measured and included in the macroscopic model). However, it is worth noting that a reduced dynamical model with an even smaller dimension could be obtained by imposing a smaller number of EFMs by means of a principal component analysis. The time evolution of some of the extracellular species is shown in the following figures where the results from step 1 (the pre-filtering which allows going from 22563 to 476 EFMs) are compared to the ones of the second cut (from 476 to 22 EFMs - or less). Fig. 4 illustrates the time evolution of lactate concentration, Fig. 5 shows the evolution of ammonia concentration and finally, Fig. 6 depicts the evolution of methionine concentration along time for the four cell cultures. The results are very satisfactory (also for the species and/or datasets not shown). For assessing the value of the approach, it is worth comparing the blue curves (step 1) to the orange ones (step 2). For most extracellular measurements, the fitting to the experimental data is identical. This allows pointing the merits of the REM algorithm which allows extracting only the most informative EFMs among the initial set. However, for a few concentration signals, slight differences may be observed as depicted in Fig. 5 and Fig. 6. Nevertheless, the results remain quite acceptable and differences can be explained by the additional tolerance required to cut the set of EFMs.

As mentioned in Sec. 3.2, the REM algorithm only ensures that the information contained in the remaining modes allows a correct reproduction of the measured data. As a matter of fact, to evaluate the sensitivity of the solution, the REM algorithm may be launched several times. In the considered application, it appears that the replication of the method with different seeds of the random number generator leads to the same set of elementary flux modes for a specific value of the threshold. When a slight difference in the latter is accepted, some variability in the selection

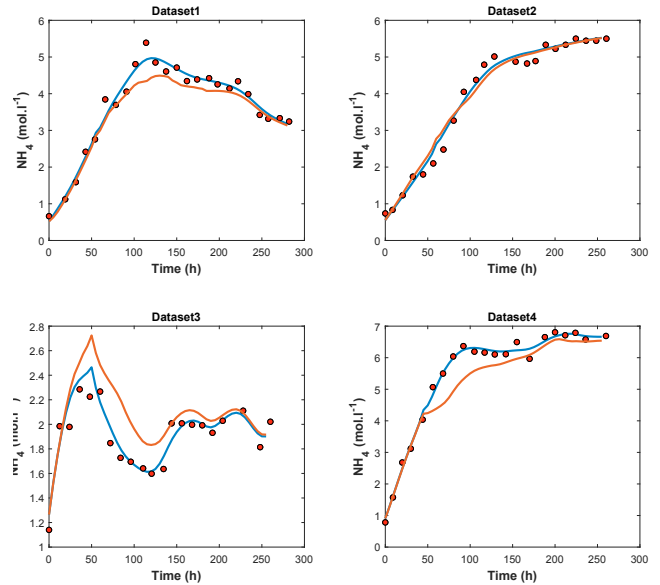


Fig. 5. Time evolution of the ammonia concentration - results of step 1 (blue line) and step 2 (orange)

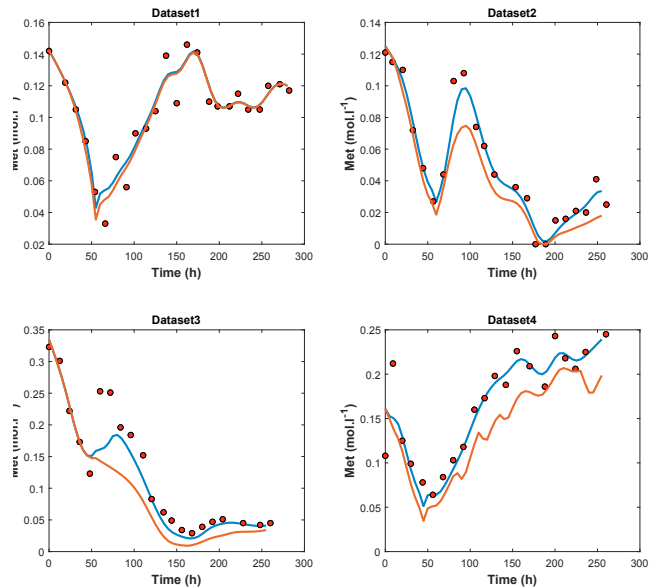


Fig. 6. Time evolution of the methionine concentration - results of step 1 (blue line) and step 2 (orange)

of the modes is noticed but the reproduction of the data is very satisfactory in all observed cases.

5-measurement case In this second case study, the whole procedure is repeated considering only five extracellular measurements, i.e. glucose, lactate, glutamine, ammonia and alanine. First, the matrix K is computed by means of Eq. 7. Second, the REM algorithm can be applied. As depicted in Fig. 1, the first step consists in estimating an approximation of SSR_q^0 . In view of the evolution of the value of the indicator and the number of remained modes shown in Table 3, 256 EFMs are considered after the pre-filtering. The last step of the algorithm is finally the definition of a target number of 5 EFMs to explain the data. The results are represented in Fig. 3. The latter

modes allow obtaining the following mass-balance dynamic model :

$$\frac{dGlc}{dt} = -\Phi_1 X - \Phi_5 X + D(Glc_{in} - Glc) \quad (13)$$

$$\frac{dLac}{dt} = \Phi_2 X - DLac \quad (14)$$

$$\frac{dGln}{dt} = -3,6926 \Phi_4 X + D(Gln_{in} - Gln) \quad (15)$$

$$\frac{dN}{dt} = \Phi_3 X - DN \quad (16)$$

$$\frac{dAla}{dt} = 2 \Phi_5 X + D(Ala_{in} - Ala) \quad (17)$$

Table 3. Results of the pre-filtering

Threshold	# EFM	SSR_q	SSR_q^0
0.980	302	2.04425×10^{-4}	
0.970	282	2.04425×10^{-4}	
0.920	256	2.04420×10^{-4}	
0.850	249	0.9059	

Another interesting observation is the comparison of the results obtained based on the two different networks for the 5 concentrations that are common to the two models. This comparison is presented in Fig. 3 for dataset 4 and shows that the EFMs inferred from the larger metabolic network allow a better reproduction of the experimental data. This motivates the use of more detailed networks to capture the observed phenotypes.

5. CONCLUSION

This work proposes a procedure for reducing an initially large set of elementary flux modes to a small subset which can be exploited to establish dynamic macroscopic models. First, the algorithm introduced in (Hebing et al., 2016) is adapted and exploited in order to eliminate the collinear EFMs. Second, the number of EFMs is further reduced to a target number by eliminating the less informative EFMs. The procedure is effective and provides promising results as illustrated in three examples. Further research entails the identification of kinetic models and the consideration of larger metabolic networks and other datasets in order to consolidate the observations and refine the algorithm.

REFERENCES

Abbate, T., Fernandes de Sousa, S., Dewasme, L., Bastin, G., and Vande Wouwer, A. (2019). Inference of dynamical macroscopic models of cell metabolism based on elementary flux modes analysis. *Biochemical Engineering Journal*, 151, 1–11.

Baroukh, C. and Bernard, O. (2016). Metabolic modeling of *c. sorokiniana* diauxic heterotrophic growth. *IFAC-PapersOnLine*, 49 (26), 330–335.

Fernandes de Sousa, S., Bastin, G., Jolicoeur, M., and Vande Wouwer, A. (2015). Dynamic metabolic flux analysis using a convex analysis approach : application to hybridoma cell cultures in perfusion. *Biotechnology and Bioengineering*, 113(5), 1102–1121.

Gao, J., Gorenflo, V., Scharer, J., and Budman, H. (2007). Dynamic metabolic modeling for a mab bioprocess. *Biotechnology progress*, 23 (1), 168–181.

Hebing, L., Neymann, T., Thüte, T., Jockwer, A., and Engell, S. (2016). Efficient generation of models of fed-batch fermentations for process design and control. *IFAC-PapersOnLine*, 49 (7), 621–626.

Jungers, R., Zamorano, F., Blondel, V., Vande Wouwer, A., and Bastin, G. (2011). Fast computation of minimal elementary decompositions of metabolic vectors. *Automatica*, 47 (6), 1255–1259.

Machado, D., Soons, Z., Patil, K.R., Ferreira, E.C., and Rocha, I. (2012). Random sampling of elementary flux modes in large-scale metabolic networks. *Bioinformatics*, 28(18), i515–i521.

Naderi, S., Meshram, M., Wei, C., McConkey, B., Ingalls, B., Budman, H., and Scharer, J. (2010). Metabolic flux and nutrient uptake modeling of normal and apoptotic cho cells. *IFAC Proceedings Volumes*, 43 (6), 395–400.

Nelson, D. and Cox, M. (2008). *LEHNINGER, Principles of Biochemistry, fifth edition*. W. H. Freeman and Company, New-York.

Niklas, J. and Heinzle, E. (2012). Metabolic flux analysis in systems biology of mammalian cells. *Genomics and Systems Biology of Mammalian Cell Culture*, Springer, 109–132.

Niu, H., Amribt, Z., Fickers, P., Tan, W., and Bogaerts, P. (2013). Metabolic pathway analysis and reduction for mammalian cell cultures - towards macroscopic modeling. *Chemical Engineering Science*, 102, 461–473.

Provost, A. and Bastin, G. (2004). Dynamic metabolic modelling under the balanced growth condition. *Journal of Process Control*, 14 (7), 717–728.

Sidoli, F., Mantalaris, A., and Asprey, S. (2004). Modelling of mammalian cells and cell culture processes. *Cytotechnology*, 44 (1-2), 27–46.

Song, H. and Ramkrishna, D. (2009). Reduction of a set of elementary modes using yield analysis. *Biotechnology and Bioengineering*, 102 (2), 554–568.

Song, H., Ramkrishna, D., Pinchuk, G., Beliaev, A., Konopka, A., and Fredrickson, J. (2013). Dynamical modeling of aerobic growth of *shewanella oneidensis*. *Metabolic Engineering*, 15, 25–33.

Soons, Z., Ferreira, I., and Rocha, E. (2011). Identification of minimal metabolic pathway models consistent with phenotypic data. *Journal of Process Control*, 21, 1483–1492.

Soons, Z., Rocha, E., and Ferreira, I. (2010). Selection of elementary modes for bioprocess control. *Computer Applications in Biotechnology*, 11, 156–161.

Stelling, J., Klamt, S., Bettenbrock, K., Schuster, S., and Gilles, E.D. (2002). Metabolic network structure determines key aspects of functionality and regulation. *Nature*, 420(6912), 190–193.

Terzer, M. and Stelling, J. (2008). Large-scale computation of elementary flux modes with bit pattern trees. *Bioinformatics*, 24(19), 2229–2235.

Vester, D., Rapp, E., Kluge, S., Genzel, Y., and Reichl, U. (2010). Virus-host cell interactions in vaccine production cell lines infected with different human influenza a virus variants : a proteomic approach. *Journal of proteomics*, 73 (9), 1656–1669.

Zamorano, F., Vande Wouwer, A.V., Jungers, R.M., and Bastin, G. (2013). Dynamic metabolic models of cho cell cultures through minimal sets of elementary flux modes. *Journal of biotechnology*, 164(3), 409–422.